Multiphoton ionization photoelectron spectroscopy of phenol: Vibrational frequencies and harmonic force field for the $^2B_1$ cation

Scott L. Anderson
Department of Chemistry, The State University of New York at Stony Brook, Stony Brook, New York 11794-3400

Lionel Goodman, Karsten Krogh-Jespersen, and Ali G. Ozkabak
Department of Chemistry, Rutgers—The State University of New Jersey, New Brunswick, New Jersey 08903

Richard N. Zare and Cheng-fa Zheng[a)]
Department of Chemistry, Stanford University, Stanford, California 94305

(Recieved 1 February 1985; accepted 14 March 1985)

A molecular beam of phenol, cooled by a supersonic expansion, is crossed at right angles by the output of a pulsed frequency-doubled dye laser, causing 1 + 1 resonance enhanced multiphoton ionization. The kinetic energy of the resulting photoelectrons is determined as a function of laser wavelength with time-of-flight analysis, permitting the assignment of 11 vibrational frequencies for the $^2B_1$ phenol-h_6 cation and ten vibrational frequencies for phenol-d_5. Of these, all but the lowest frequency one in each case are in-plane vibrations of which phenol has a total of 19. An approximate harmonic force field for the in-plane modes of the phenol cation is derived along with its associated frequencies and mode forms. This in turn facilitates the vibrational analysis. Analogous force field calculations have been carried out on the ground ($^1A_1$) and first excited ($^1B_2$) states of the neutral parent, permitting conclusions to be reached concerning bonding changes upon removal of an electron from the phenol electron system.

I. INTRODUCTION

The set of vibrational frequencies associated with a particular electronic state contains considerable information about the geometrical and electronic structure of the molecule. They define the shape of the potential energy surface near the equilibrium geometry of the state, and for this reason vibrational spectroscopy has long been an extremely active field.[1-4] One major class of molecules for which comparatively little vibrational data are available is molecular ions, because experimental difficulties hinder the application of traditional spectroscopic methods. In recent years this situation has improved considerably, particularly for small molecular ions, due to the development of sensitive laser techniques such as fluorescence,[5,6] optical–optical double resonance,[7] infrared difference-frequency laser spectroscopy,[8,9] velocity modulation infrared laser spectroscopy,[10] and indirect laser-beam ion-beam methods.[11,12] Nevertheless, for medium (e.g., benzene) to large molecular ions, almost all the vibrational data available continues to come from photoelectron spectroscopy (PES).[13-15]

Although conventional single-photon PES is a powerful tool for studying photoionization dynamics and the electronic structure of ions and their neutral precursors,[16] there are several serious drawbacks to its use in vibrational spectroscopy. First, photoelectron spectroscopy is inherently a low resolution technique compared to optical spectroscopy, which makes resolution and interpretation of congested spectra difficult. Second, ionization Franck-Condon factors often favor the population of only a few, usually totally symmetric, vibrational modes.[14] Consequently, only a restricted number of vibrational frequencies can be found and in the case of medium to large polyatomic ions with many vibrational modes, the assignments are often no more than educated guesses. Recent work of Reilly *et al.*[17] and Anderson *et al.*[18] using resonance enhanced multiphoton ionization (MPI) as the ionization source for photoelectron spectroscopy suggest that MPI has the capability of greatly increasing the amount of vibrational information obtainable from photoelectron spectroscopy. In this paper we report an MPI-PES study of the phenol ($C_6H_5OH^+$) and phenol-d_5 ($C_6D_5OH^+$) cations which demonstrates the power of this technique.

Determination of many experimental frequencies has allowed us to construct an approximate harmonic force field for the in-plane modes of the cationic ground state ($^2B_1$ in C_{2v} symmetry). This force field with its associated frequencies and mode forms in turn facilitates the interpretation of the spectra. In addition, analogous force field calculations on the ground ($^1A_1$) and first excited singlet [^1L_b ($^1B_2$)] states of the neutral species have been carried out for comparison purposes. In presenting and discussing these fields, we direct our primary attention to comparing the vibrational structure (force constants, frequencies, and mode forms) of the cation with those of the ground and excited state of the neutral species. This comparison of potential energy surfaces serves to illuminate some basic ideas about bonding derived from electronic structure theory.

The excitation/ionization scheme used for MPI-photoelectron spectroscopy is depicted in Fig. 1. Neutral precursor molecules are cooled in a supersonic jet so that most molecules are in the vibrationless ground state. Single pho-

[a)] Present address: Nuclear Science Department, Fudan University, Shanghai, People's Republic of China.

 0021-9606/85/125329-11$02.10

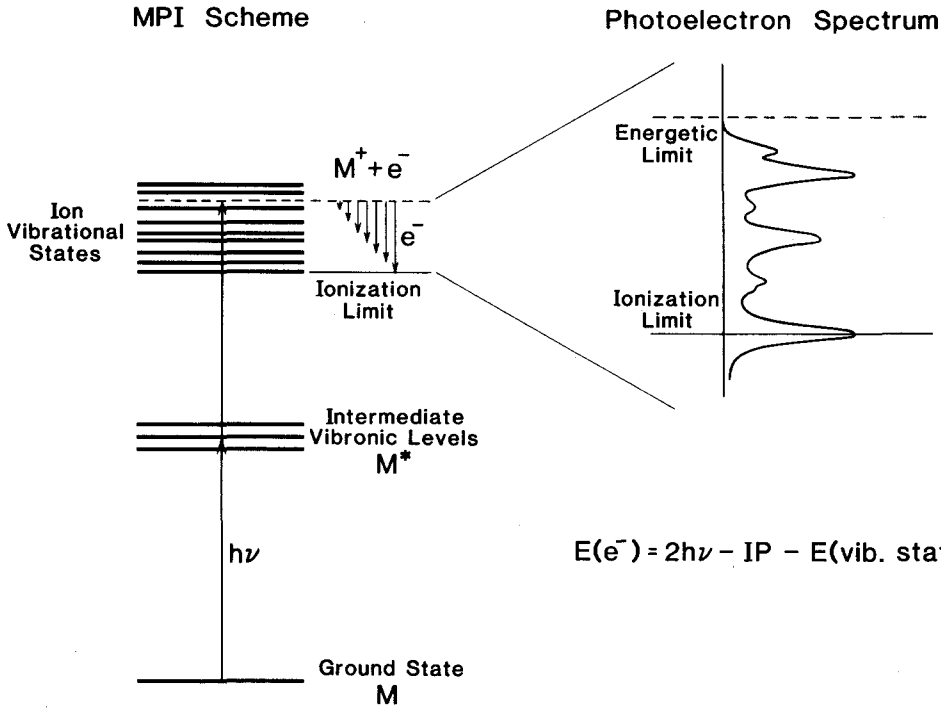

FIG. 1. MPI-PES energetics showing the relation between photon energy and the photoelectron energy spectrum.

ton excitation at moderate power levels pumps some molecules to a known vibrational level of the first excited singlet state. On the average, the excited molecules spend many vibrational periods in this state before a fraction are ionized by absorption of a second photon. Kinetic energy analysis of the photoelectrons allows measurement of the energies and population distributions of the various vibrational levels of the ion which lie below the combined energy of the two absorbed photons. Due to the relatively long-lived nature of the actual intermediate state, it is conceptually useful to consider the entire ionization process as a single-photon ionization where the lower level is an excited state which can be varied by tuning the exciting laser to different frequencies. The ionization Franck–Condon factors are those appropriate to the excited state to ion transition and can also be varied by tuning the laser. Herein lies the greatest advantage to using MPI for photoelectron spectroscopy. Instead of obtaining just a single spectrum for each ion, a new spectrum is generated for each intermediate vibronic level pumped by the laser. Thus, even if the individual spectra were no better than those obtained in single-photon ionization, the large number of spectra increases the potential information content considerably.

Phenol was chosen for a number of reasons. The UV absorption to the first excited singlet state is in a convenient spectral range and the MPI signal is very strong. The IR and UV absorption spectra have been well characterized; in particular, Bist, Brand, and Williams (hereafter referred to as BBW) have carried out a very complete study of the h_6, d_1, and d_5 isotopes of phenol leading to essentially complete assignments of all 33 vibrational modes in both the ground and first excited singlet states.[19] Rava and Goodman[20] have recently studied two-photon excitation to the first excited singlet state and made some modifications to the vibrational assignments proposed by BBW. The strong electrostatic perturbation by the hydroxy group produces substantial splitting of the degenerate benzene frontier—π orbitals.[15] Thus, it appears reasonable to neglect the Jahn-Teller effects present in the benzene cation[17(b)] and discuss the phenol cation in terms of a well-defined harmonic surface with just a single minimum. The two ingredients applied to elucidate features of the phenol surface, MPI photoelectron spectroscopy and force field calculations, complement each other and provide detailed information about structure and bonding in the phenol cation. An example of the importance of such information is the study of the phenol cation decomposition, where vibrational structural data are used in statistical modeling of unimolecular dissociation process.[21]

II. EXPERIMENTAL

These experiments were carried out using a MPI-PES spectrometer developed at Stanford University. The laser source for these experiments is a Quanta-Ray ND:YAG pumped dye laser operating with either rhodamine 590 or coumarin 500 dye. The dye laser output is frequency doubled in a homemade autotracking doubling setup, and can either be used directly or Raman shifted in H_2 to shorter wavelengths.

Typical pulse energies are 200–500 μJ. Higher powers are easily achieved but are found to result in broadened spectra. In order to reduce space charge broadening effects the laser is focused rather loosely with a cylindrical lens (25 cm fl) resulting in power densities in the MW/cm^2 range. Because the photon energies involved ($\sim$4.5 eV) are sufficient to cause photoemission from both the flight tube and the electron multiplier, it is necessary to baffle the laser beam carefully.

The time-of-flight (TOF) photoelectron spectrometer used in this work is shown in Fig. 2. It consists of an 8 cm i.d.

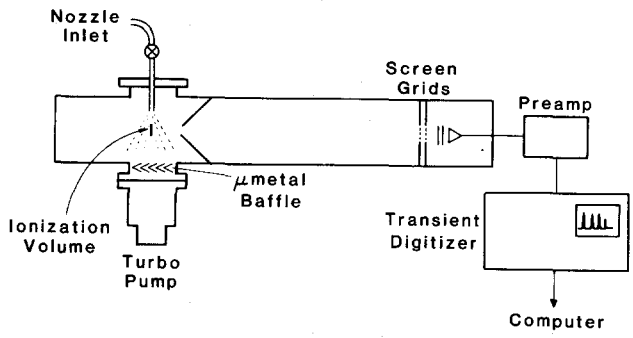

FIG. 2. Schematic of the MPI-PES spectrometer.

double wall mu-metal flight tube contained in a stainless steel vacuum chamber evacuated by a 110 ℓ/s turbo molecular pump. All surfaces on the inside of the flight tube are graphite coated to help maintain a uniform surface potential. In addition, the entire instrument can be baked to 250 °C when necessary for cleaning. Ultimate pressure is 2×10^{-9} Torr with 2×10^{-8} Torr background pressure typical. Measured magnetic field strength on axis is <1 mG in the flight tube and ~5 mG in the ionization region, where the mu-metal shield is perforated to allow the laser and molecular jet to pass through. A conical mu-metal baffle separates the ionization region from the flight tube and also serves to reduce the background signal from scattered photoelectrons and laser light. Good magnetic shielding and clean vacuum conditions are essential for successful operation.

Phenol-h_6 (Aldrich) was used without purification. Phenol-d_5 was made from phenol-d_6 by proton exchange in H_2O followed by extraction and vacuum sublimation. The gas sample is admitted to the spectrometer in a pulsed free jet expansion using a low current piezoelectric pulsed valve (Lasertechnics).

Typical operating conditions are: nozzle diameter 0.3 mm; nozzle–interaction region distance 5 cm; 0.2 Torr phenol seeded in 200–800 Torr Ar, pulse length 200 μs, rep. rate 10 Hz, time averaged background pressure $<2\times10^{-6}$ Torr, estimated total pressure in interaction region 10^{-3} Torr. The laser is triggered 50 μs after the leading edge of the gas pulse reaches the interaction volume. In this way the entire photoelectron TOF distribution is recorded before the neutral beam molecules scatter into the flight tube. The ionization volume is defined by the intersection of the loosely focused laser beam with the free jet and is centered on the axis of the flight tube about 3 cm from the end of the conical baffle.

The electron detector, a channel electron multiplier array with 50 Ω anode (Galileo FTD2003) is located at the opposite end of the flight tube, separated from the field-free region by a double shielding grid. The field-free flight path is 50 cm. No collection or accelerating fields are used in the spectrometer; thus the collection efficiency (5×10^{-4}) is determined by the solid angle subtended by the detector. Electron TOF distributions were obtained by recording the amplified detector output with a Tektronix 7912 AD transient digitizer operating at a 3.9 ns/channel sweep rate. The laser power was adjusted to limit signal levels to 10-20 counts/shot since space charge broadening sets in at higher signal levels. Spectra are corrected for scattered light signal by subtracting TOF spectra obtained with the pulsed beam on and off, each signal averaged for $\sim10\,000$ laser shots. Raw signal-to-background (photoelectron and scattered light) ratios are typically 5. Resolution in these spectra ranges from 10–15 meV FWHM, depending on electron energy. This is not the timing resolution limit for the instrument (2 meV) and is presumably due to residual electric and magnetic fields and unresolved rotational structure.

A. TOF-energy inversion

In principle it is trivial to convert a time-of-arrival distribution to an energy distribution thus:

$$E=\frac{mv^2}{2}=\frac{mN(t)}{2}\left[\frac{L}{(t-t_0)}\right]^2,$$

where L is the flight path, t is time of arrival, t_0 is the time when the laser fires, m is the mass of the electron, and $N(t)$ is a normalization function which keeps relative peak areas constant in the inversion. This simple inversion assumes no stray fields in the instrument and is quite satisfactory at high electron energies. Initial experiments in this laboratory[18] used this expression (without the normalization factor) for TOF-energy conversion. $2+1$ photon ionization of xenon through the $6p[3/2]_2$ and $6p[1/2]_0$ states was used to generate a total of three calibration peaks which were fit to yield the two slightly adjustable parameters in the inversion function, L and t_0. The problem with this procedure is that all the xenon calibration peaks appear at high electron energy (>1.46 eV), and it is not a valid assumption, for our instrument at least, to assume that the energy scale determined in this way is accurate at low electron energies. For the case of the chlorobenzene MPI-PES published previously,[18] the vibrational frequencies given (which are differences between photoelectron band positions) are accurate within the reported error limits because the energy spacing are small and nonlinearities in the energy scale have minimal effect. In the present case, where the electron energy range of the experiment is larger and we are striving for increased accuracy, it has become necessary to find an improved way to calibrate. Two basic techniques are used.

$Fe(CO)_5$ is easily photolyzed by UV light to bare iron atoms.[22] At the wavelengths and power densities used in the MPI-PES studies reported here, the atoms are mostly formed in the ground $a\,^5D$ and first excited $a\,^5F$ manifolds. As the laser is tuned, atoms are very efficiently $1+1$ photon ionized at a large number of atomic absorption lines. Photoelectron spectra of atomic iron are thus easily obtained and in many cases yield well resolved peaks of well known energies. An example of the photoelectron spectrum taken at a particular resonance line is shown in Fig. 3. Since there are a large number of atomic absorptions in each of the dye ranges used in these experiments, it is simple to generate five or more calibration peaks which span the energy range from ~0.2 to 2 eV. Fitting to these peaks thus insures a highly accurate and linear energy scale.

It is possible to ionize xenon by a $2+1$ photon process when using rhodamine 590 for the longer wavelength portions of this experiment. The appropriate photon frequency is obtained by Raman shifting the doubled dye (DD) laser

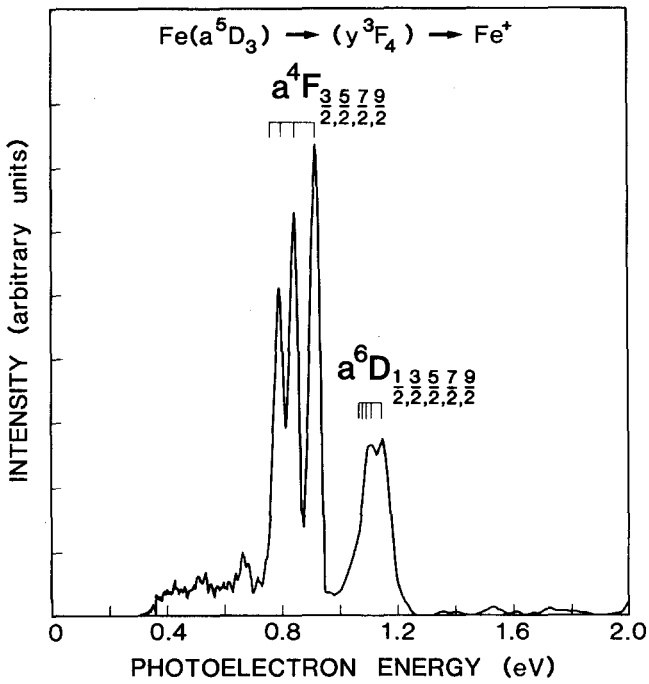

FIG. 3. Typical MPI photoelectron calibration spectrum of atomic iron following photolysis of $Fe(CO)_5$.

output in H_2 and using the first anti-Stokes line (AS_1). If instead of using only AS_1, all orders from the Raman cell are focused into the spectrometer, a series of photoelectron peaks is obtained corresponding to excitation by 2 AS_1 with subsequent ionization by S_2, S_1, DD, AS_1, AS_2, AS_3, and AS_4. These peaks, which are separated by 4155 cm^{-1}, span the electron energy range from 1.2 to 4.3 eV; thus this technique is particularly useful for calibrating the higher energy part of the photoelectron spectrum.

In either case, a four "slightly adjustable" parameter fit is used in the TOF-energy inversion. The functional form is

$$E=\frac{mN(t)}{2}\left[\frac{L}{(t-t_0)}\right]^2+\frac{b}{(t-t_0)}+c\,.$$

As above, L and t_0 are slightly adjustable and account for variations in flight path due to inhomogeneous fields as well as timing uncertainties. The c term has the physical significance of an energy shift due to stray electric fields and the b term is a correction factor. When the instrument is operating well, L and t_0 are within 5% of the measured values and b and c are close to zero. For the spectra reported here the energy scale is precise and linear to <1 meV in the case of phenol-h_6 and <1.5 meV for phenol-d_5.

The accuracy of the reported vibrational frequencies is lower however, due to two factors. First, the observed band shapes are often asymmetric which makes determination of the band center difficult. This problem is partially offset by the fact that all the bands are shaded to lower energies and inaccuracies in absolute energy tend to cancel in measurements of band spacings. A second problem is that bands are observed to shift with varying laser power and signal intensity. These shifts, which are presumed to be due to space charge, are small (~ 1 meV) for the high energy photoelectron bands and increase with decreasing photoelectron energy to about 4 meV for the lowest energy bands used in determining vibrational frequencies. The reason for the variation of shift with photoelectron energy is that the high energy bands are due to fast electrons which leave the charge cloud in the ionization volume while it is still nearly neutral. Lower energy electrons, on the other hand, are retarded by the increasingly positive charge cloud left behind by the faster electrons. Consequently, higher vibrational frequencies are less accurately determined than lower ones. Since it is not clear how to correct for this effect, we merely estimate the error in the reported vibrational frequencies to be ± 1.5 meV or $\pm 2\%$, whichever is greater. (Note 1 meV = 8 cm^{-1}.)

B. Representative spectra

A total of 26 different photoelectron spectra for phenol were recorded representing one plus one photon ionization through various resonant vibronic levels of the first excited singlet ($^1B_2$) state. Rather than report all these spectra, we will present a few to demonstrate the trends observed and then tabulate the frequencies derived from the spectra.

Figure 4 shows photoelectron spectra resulting when four different transitions are pumped. In each case no hot bands are observed and the highest kinetic energy feature is the origin.

The first spectrum results from pumping through the vibrationless level of the $^1B_2$ state. The most intense peak in the photoelectron spectrum corresponds to formation of phenol cations in the vibrationless ground state (photoelectron energy of 0.514 eV). Peaks at lower photoelectron energy correspond to vibrationally excited ions and have been labeled by their spacing from the origin band.

The three other spectra are all different from each other and from the spectrum arising from the vibrationless level. However, they do show a pattern which is common to many phenol-h_6 photoelectron spectra. When ionization is through a particular intermediate vibronic level of the singlet state, the photoelectron spectra has a prominent progression in an ion vibrational mode with about the same frequency. Usually the member of the progression with one quantum of excitation is most intense. The rest of the spectrum consists of short progressions of other modes, usually in combination with one or more quanta of the dominant mode. Assignment of the spectra can be made easily and with some confidence, since the origin-to-dominant peak spacing in each spectrum yields one unique ion fundamental frequency. Once these are known, the assignment of the rest of the peaks is straightforward and confirms the vibrational frequencies.

Unlike phenol-h_6, where each spectrum looks quite different, the same spectrum of three large peaks and several small ones is obtained for phenol-d_5 (Fig. 5), independent of which intermediate vibronic level is pumped. The only difference is that the set of peaks appears shifted by a spacing which corresponds to the frequency in the ion of the mode which was pumped in the intermediate state. Again, one ion fundamental frequency can be extracted from each photoelectron spectrum. Unfortunately, these simple vibrational patterns begin to break down when modes of frequency larger than 1200 cm^{-1} are pumped in the intermediate state. At

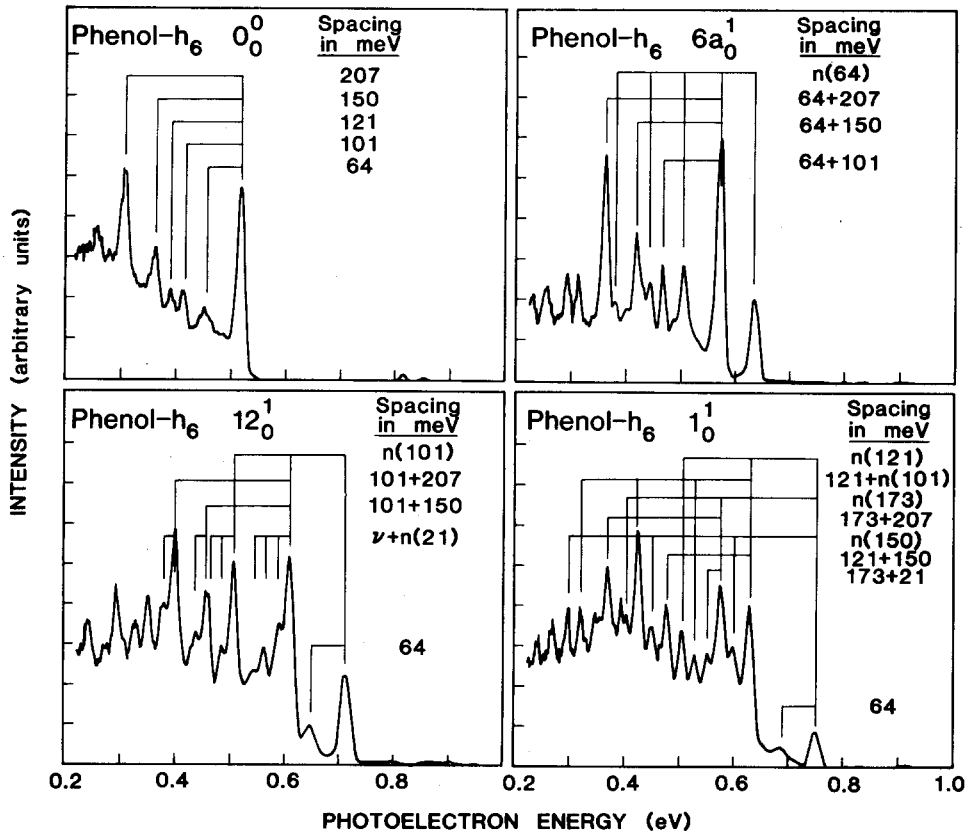

FIG. 4. Representative MPI-PES spectra of phenol-h_6. Note the prominent progression in the mode excited in the intermediate state.

that point two effects complicate matters. First, spectral congestion makes resolution of peaks difficult; in addition, the correlation between the mode pumped in the intermediate state and the dominant progression in the ion vibrational distribution breaks down. It is still possible to assign the spectra, but no fundamentals above 1700 cm^{-1} are seen. While we are reasonably confident of the assignments given, there are two reported frequencies which are close enough to

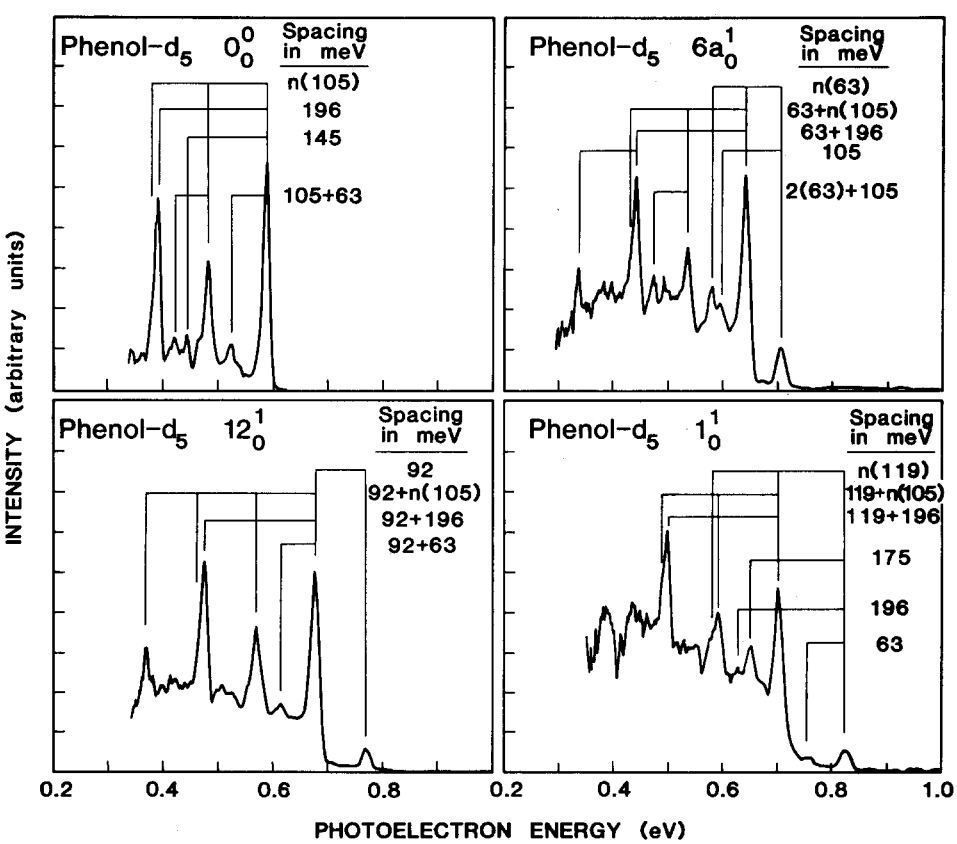

FIG. 5. Representative MPI-PES spectra of phenol-d_5. Note recurrence of vibrational pattern.

TABLE I. Measured phenol ion vibrational frequencies (cm^{-1}).

Ion frequency $^2B_1$	Phenol-h_6 Frequency in neutral[a] $^1A_1$	$^1B_2$
1669	...	...
1500	...	...
1395	1261.5	1273.2
1210	1168.9	975.0
1040	1072.4	961.7
1027	1025.9	957.6
976	999.3	934.8
815	823.2	782.7
556	619.2	522.8
516	526.6	475.1
169[b]	408.0	187.0
	Phenol-d_5	
1581	...	...
1565	...	...
1174	...	...
960	960.2	926
851	879.1	840.6
744	754	718.6
508	512.6	463
428	594.9	500.6
395	385	377.7
129[b]	357.4	147

[a] Frequencies from Refs. 19 and 20.
[b] Out-of-plane, probably ring torsion.

twice the energy of a lower frequency vibration to cause some doubt as to whether they are indeed fundamentals. These are the 207 meV vibration in phenol-h_6 and the 196 meV vibration in phenol-d_5, which are close to double the 101 and 105 meV bands, respectively. In both cases assignment as harmonics would require large anharmonicities and unexpected Franck–Condon envelopes. In the case of the 196 meV frequency in phenol-d_5, assignment as a fundamental is further strengthened by the results of the normal mode calculation discussed below.

A summary of the measured ion vibrational frequencies is given in Table I. In cases where there is a clear association between the ion vibration and the vibration pumped in the intermediate state, the frequencies in the neutral ground and intermediate states are given for comparison.

III. FORCE FIELD CALCULATIONS

In an attempt to rationalize the appearance of the cation vibrational spectra we have carried out force field calculations using a revised version of the computer programs developed by Schachtschneider.[23] The vibrational secular equations are solved via the Wilson FG matrix formalism[2] with molecular geometry, atomic masses, and a set of force constants as input. Output consists of calculated frequencies and normal mode displacements (Q_i). It is possible to carry out a least squares iterative fit between experimental and calculated frequencies to achieve a set of optimal force constants.

The low symmetry of phenol (C_s) implies that to construct an accurate force field for just the in-plane modes would require a very large number of force constants. The out-of-plane modes are relatively unimportant for the spectra and will not be dealt with further. There are many fundamental frequencies known for the ground and first excited singlet state of phenol and deuterated phenols[19] and we have, in fact, established elaborate force fields for these states containing 38 distinct force constants. A similar extensive treatment of the cation was attempted but failed because an insufficient number of experimental ion frequencies was available. Convergence to a set of unique, physically satisfactory force constants could not be achieved despite numerous attempts. Instead, we resort here to a perturbation model in which phenol is treated as a mass perturbed benzene.

The model approximates the OH group by a single atom X with the combined mass of an oxygen and a hydrogen atom. The C_6H_5X neutral and ionic species thus have C_{2v} symmetry, which is reasonable in light of the fact that the rotational barrier for the phenolic OH group is very small (1200 cm^{-1}).[24] Also, the vibrational features in the lowest singlet excited state of neutral phenol are clearly well described using C_{2v} symmetry designations.[19,20] The experimental ground state geometry for benzene was used for C_6H_5X throughout.[25] The force fields for C_6H_5X are based on the approach taken by Kydd for the benzene ground state.[26] The Kydd force field for the in-plane modes is expressed in terms of internal coordinates (t_i for CC stretch, s_i for CH stretch, α_i for CCC angle bend, and β_i for CH rocking) and contains 17 constants.[26,27] To this force field a separate force constant for the C–X stretch was added so that our force fields contain a total of 18 force constants for each phenol neutral or ionic state.

A value for the C–X ground state stretching constant was determined by optimization to the observed phenol ground state infrared frequencies using Kydd's benzene values for all the remaining force constants. The optimized value (6.198 mdyn/Å, Table II) actually compares well with the

TABLE II. Comparison of ground, excited state, and cation force constants.[a,b]

Force constant	Ground state	Excited state	Cation
t_it_i (C–C str.)	7.040	6.233	6.551*
s_is_i (C–H str.)	5.061	5.120	5.090*
s_1s_1 (C–O str.)	6.198*	6.959*	7.582*
$\alpha_i\alpha_i$ (CCC bend)	1.103	1.041	1.076*
$\beta_i\beta_i$ (CH rock)	1.020	0.940	1.033*
t_it_{i+1}	0.650	−0.127	0.395*
t_it_{i+2}	−0.609	0.094	0.041*
t_it_{i+3}	0.295	0.383	0.873*
s_is_{i+2}	0.034	0.068	0.050
$\alpha_i\alpha_{i+1}$	−0.097	−0.085	−0.090
$\beta_i\beta_{i+1}$	0.028	0.014	0.020
$\beta_i\beta_{i+2}$	−0.015	0.009	−0.010
$\beta_i\beta_{i+3}$	−0.032	−0.022	−0.030
α_is_i	−0.014	0.420	−0.737*
α_it_i	0.602	0.208	0.028*
$\beta_i\alpha_{i+1}$	−0.063	−0.135	−0.100
$t_i\beta_i$	−0.315	−0.408	−0.360
$t_i\beta_{i+3}$	−0.027	0.007	0.010

[a] Stretch constants are in mdyn/Å, bend constants are in mdyn Å/rad, and stretch bend constants in mdyn/rad.
[b] Optimized force constants from the phenol spectra are designated by *.

typical C-O stretching constant for aliphatic carboxylic acids.[28] The phenol excited state constants were the optimal set recently determined by Krogh-Jespersen *et al.* for the first excited singlet state ($^1B_{2u}$) of benzene[29] augmented with a C–X stretching constant (6.959 mdyn/Å) optimized analogously to the known excited state frequencies.[19,20]

A total of ten force constants were optimized in the cation. They included all five diagonal force constants and the major off-diagonal interaction constants involving the skeletal portion of the molecule, i.e., the region of electron loss. Values of the remaining eight force constants were the average of the ground and excited state values. The actual values for several of the optimized diagonal constants are in fact also well approximated by the means of the ground and excited state values (Table II).

Within the constraints of our mass perturbation model the ring portion of the molecule is identical in phenol and in benzene; and therefore the ring force constants are equivalent. Since an accurate force field is available for both the ground state[25] and $^1B_{2u}$ excited state[28] of benzenes we have used these force constants for the ring. The benzene cation force constants are not known and furthermore Jahn–Teller effects will prevent the benzene cation from serving as an appropriate model for a harmonic force field for the phenol cation. Therefore, we have generated an optimized cation force field using phenol photoelectron spectra.

A few points may be made regarding the values of the optimized force constants as they relate to the electronic structure of the cation. Simplistically, the cation is generated by removal of an electron from the highest occupied molecular orbital (HOMO) of neutral phenol; similarly, the neutral excited state consists of electron promotion from this HOMO into the lowest unoccupied molecular orbital (LUMO). Both these orbitals are π type and the molecular orbital coefficients are shown in Fig. 6.[30] The phenol HOMO is the $e_{1g}(a)$ HOMO orbital of benzene with a large oxygen contribution mixed in, whereas the phenol LUMO is the virtually unchanged $e_{2u}(b)$ LUMO orbital of benzene.[31] The overall effect of π ionization or occupation of the "antibonding" LUMO is clearly to diminish the bonding in the ring as evidenced, for example, by the frequency reduction of the ring mode ν_6[17(b)] upon ionization of benzene or by the ring expansion (0.044 Å) observed upon excitation to the $^1B_{2u}$ state.[32] Thus, the averaged CC stretch constant ($t_i t_i$, Table II) decreases upon molecular ionization from its ground state value of 7.040 to 6.551 mdyn/Å and even further to 6.233 mdyn/Å as the result of electronic excitation. In contrast, the CO stretch constant increases in value in the ionized species from both the neutral ground and excited states. It is nearly 25% larger in the cation than in the neutral ground state. This arises from the fact that the HOMO is strongly antibonding across the C–O linkage, thus π ionization out of this orbital effectively increases CO bonding. Direct geometry optimization for the ground state of neutral phenol and its cation using *ab initio* Hartree–Fock molecular orbital theory and the STO-3G basis set shows a decrease in the CO bond length of 0.082 Å and an average increase of 0.035 Å in CC bond length upon ionization,[30(b)] in full accord with the changes in force constants obtained empirically in the force fields. The large cation value for the para CC-stretch interaction constant ($t_i t_{i+3}$) may also reflect the orbital composition of the HOMO, which shows strong destabilizing 1,4 interactions across the phenyl ring. Removal of an electron from the HOMO would relieve some of the 1,4-antibonding character, effectively increasing the bonding diagonally across the ring.

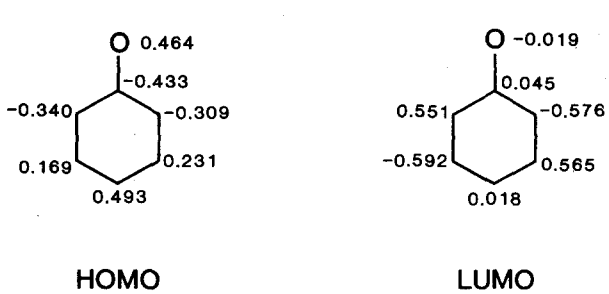

FIG. 6. Calculated phenol HOMO and LUMO $2p(\pi)$ coefficients.

The basic rationalization for the perturbation approach is that the phenol spectra to a large extent have their roots in the benzene spectra. It is not at all surprising that the more extensive calculations reproduce the frequencies more accurately than the perturbation model (e.g., the average discrepancy for the ground state is 3 vs 18 cm^{-1}), but the latter model has the advantage of being far more amenable to physical interpretation. We can perform an internally more consistent treatment of the cation and neutral molecule states, and interpret force constant changes more readily in terms of electronic structure changes. An additional advantage to the perturbation model arises from the fact that since the benzene modes span the same space as the C_6H_5X modes, we can express all the calculated C_6H_5X modes as linear combinations of benzene modes, viz.

$$Q_j^{C_6H_5X} = \sum_i a_{ij} Q_i^{C_6H_6}.$$

For internal consistency, the phenol neutral, excited, as well as ionic state modes have all been expressed in terms of the benzene ground state modes calculated with the Kydd force field. The expansion coefficients a_{ij} are shown in Tables III–V. We will use the labeling introduced by Wilson[2] to denote the benzene ground state modes (Q''_1, Q''_{6a}, Q''_{18b}, etc.); diagrams for these modes may be found in Fig. 1 of Ref. 29. The mode decompositions enable us to trace the origins of the phenol modes. Inspection of Tables III–V shows immediately that most phenol modes are of very mixed character and do not correspond uniquely to particular benzene modes. Consequently, we will only use the Wilson labels for the benzene modes.

The most glaring disadvantage to the perturbation model is of course that since the H atom of the OH group is neglected, two in-plane frequencies are not predicted from the calculations. One of the missing modes is the O–H stretch, which has a fundamental frequency in excess of 3600 cm^{-1} and thus falls in a region where no data are available in either the cationic or UV spectra, nor are there any other fundamentals in that region. The second missing mode cor-

TABLE III. Mode decomposition for the phenol ground state.[a]

ν^b	Symmetry	
1640	a_1	$0.83\,Q''_{8a}$
1578	b_2	$0.99\,Q''_{8b}$
1515	a_1	$0.48\,Q''_{8a} + 0.82\,Q''_{19a}$
1438	b_2	$0.89\,Q''_{19b} + 0.38\,Q''_{3}$
1328[c]	a_1	$0.47\,Q''_{19a} - 0.34\,Q''_{18a} + 0.38\,Q''_{12} + 0.34\,Q''_{1}$
1321	b_2	$0.80\,Q''_{3} + 0.44\,Q''_{14}$
1278	b_2	$0.88\,Q''_{14} + 0.31\,Q''_{9b}$
1167	a_1	$1.00\,Q''_{9a}$
1155	b_2	$0.56\,Q''_{9b} - 0.83\,Q''_{15}$
1060	b_2	$0.37\,Q''_{9b} + 0.87\,Q''_{18b}$
1023	a_1	$0.81\,Q''_{18a} + 0.58\,Q''_{12}$
995	a_1	$0.56\,Q''_{12} - 0.77\,Q''_{1}$
802	a_1	$0.31\,Q''_{18a} - 0.39\,Q''_{12} - 0.47\,Q''_{1} + 0.57\,Q''_{6a}$
618	b_2	$0.98\,Q''_{6b}$
489	a_1	$0.77\,Q''_{6a}$
383	b_2	$0.31\,Q''_{19b} - 0.50\,Q''_{9b} - 0.33\,Q''_{15} + 0.40\,Q''_{18b}$

[a] Decomposition is in terms of benzene ground state modes calculated with the Kydd force field (Ref. 26) (Wilson numbering) (Ref. 2). Of the 21 in-plane modes, the five highest frequency ones (corresponding to C–H stretching vibrations) are excluded. Only components with coefficients > 0.30 are given.
[b] Calculated frequencies in cm^{-1}.
[c] Believed to be severely in error due to missing bending mode in the perturbation model calculation.

responds to the HOC bend in the 1000–1200 cm^{-1} region. There are other fundamentals present in this frequency range, and the largest errors incurred by the perturbative procedure can thus be expected to involve frequencies and modes in this region.

A. Neutral phenol states

Primarily as a result of the mass perturbation, several phenol ground state modes have only minor resemblance to pure benzene modes (Table III). Four modes have major C–O motions. The 802 and 489 cm^{-1} modes have large oxygen stretching motion and may be considered to arise from substituent (X)-sensitive benzene modes Q''_{12} and Q''_{6a}. The low frequency mode at 383 cm^{-1} may be considered as the CO bend and arise from X-sensitive benzene mode Q''_{18b}. The 1328 cm^{-1} mode may be interpreted as C–O stretch. The large error (66 cm^{-1}) in its calculated frequency relative to the observed value (1262 cm^{-1}) is believed to be due to the absence of the OH bending mode in the calculation. If this large discrepancy is ignored, the average absolute error is 15 cm^{-1} between observed and calculated values, providing support for the validity of treating phenol as a C_6H_5X species.

TABLE IV. Mode decomposition for the phenol excited state.[a]

ν^b	Symmetry	
1673	a_1	$0.33\,Q''_{20a} + 0.69\,Q''_{8a}$
1570	b_2	$0.96\,Q''_{14}$
1524	b_2	$0.99\,Q''_{8b}$
1433	a_1	$0.64\,Q''_{8a} + 0.64\,Q''_{19a}$
1345	b_2	$0.78\,Q''_{19b} + 0.61\,Q''_{3}$
1298	a_1	$0.72\,Q''_{19a}$
1273	b_2	$0.46\,Q''_{19b} - 0.71\,Q''_{3} + 0.43\,Q''_{9b} + 0.31\,Q''_{15}$
1147	b_2	$0.58\,Q''_{9b} - 0.79\,Q''_{15}$
1142	a_1	$0.98\,Q''_{9a}$
974	b_2	$0.35\,Q''_{9b} + 0.87\,Q''_{18b}$
941	a_1	$0.50\,Q''_{18a} + 0.78\,Q''_{12} - 0.37\,Q''_{1}$
924	a_1	$0.68\,Q''_{18a} + 0.73\,Q''_{1}$
747	a_1	$0.39\,Q''_{18a} - 0.42\,Q''_{12} - 0.45\,Q''_{1} + 0.51\,Q''_{6a}$
558	b_2	$0.95\,Q''_{6b}$
436	a_1	$0.80\,Q''_{6a}$
358	b_2	$0.48\,Q''_{9b} + 0.31\,Q''_{15} - 0.40\,Q''_{18b}$

[a] Decomposition is in terms of benzene ground state modes calculated with the Kydd force field (Ref. 26) (Wilson numbering) (Ref. 2). Of the 21 in-plane modes, the five highest frequency ones (corresponding to C–H stretching vibrations) are excluded. Only components with coefficients > 0.30 are given.
[b] Calculated frequencies in cm^{-1}.

TABLE V. Mode decomposition for the phenol cation ground state.[a]

ν^b	Symmetry	
1672	a_1	$0.88\,Q''_{8a}$
1627	b_2	$0.99\,Q''_{8b}$
1515	a_1	$0.36\,Q''_{8a} + 0.83\,Q''_{19a}$
1434	b_2	$0.87\,Q''_{19b} + 0.39\,Q''_{3}$
1393	b_2	$0.94\,Q''_{14}$
1351	a_1	$0.51\,Q''_{19a} + 0.42\,Q''_{1}$
1321	b_2	$0.82\,Q''_{3} - 0.40\,Q''_{9b}$
1189	a_1	$1.00\,Q''_{9a}$
1187	b_2	$0.57\,Q''_{9b} - 0.80\,Q''_{15}$
1037	b_2	$0.36\,Q''_{9b} + 0.88\,Q''_{18b}$
1016	a_1	$0.54\,Q''_{18a} - 0.37\,Q''_{12} + 0.75\,Q''_{1}$
988	a_1	$0.65\,Q''_{18a} + 0.75\,Q''_{12}$
801	a_1	$0.40\,Q''_{18a} - 0.44\,Q''_{12} - 0.43\,Q''_{1} + 0.42\,Q''_{6a}$
561	b_2	$0.96\,Q''_{6b}$
479	a_1	$0.87\,Q''_{6a}$
381	b_2	$0.48\,Q''_{9b} + 0.32\,Q''_{15} - 0.40\,Q''_{18b}$

[a] Decomposition is in terms of benzene ground state modes calculated with the Kydd force field (Ref. 26) (Wilson numbering) (Ref. 2). Of the 21 in-plane modes, the five highest frequency ones (corresponding to C–H stretching vibrations) are excluded. Only components with coefficients > 0.30 are given.
[b] Calculated frequencies in cm^{-1}.

The excited state force field reproduces the experimental frequencies of the two ring isotopic phenols for which data are available (C_6H_5OH and C_6D_5OH) with an absolute average error of 23 cm^{-1}. From direct comparisons of the nuclear displacements (Figs. 7 and 8), four modes are predicted to undergo large changes in form between the phenol ground and excited state, i.e., Duschinsky rotation.[33] The pair of b_2 modes with excited state frequencies at 1273 and 1570 cm^{-1} are calculated to arise predominantly from Q''_3 and Q''_{14} and their mode pictures are given in Figs. 7 (top) and 8 (bottom), respectively. The b_{2u} mode Q''_{14} is a Kekulé-type mode describing alternating expansion and compression of the ring, whereas the a_{2g} mode Q''_3 involves motions of the carbon and hydrogen atoms in a counter-rotatory manner.[29] The mode diagram for the 1570 cm^{-1} mode in phenol is virtually identical with that of the 1568 cm^{-1} mode in benzene (Ref. 29, Fig. 2, Q'_{14}) with only pure skeletal CC motion being present. The pair of a_1 symmetry modes with excited state frequencies of 941 and 924 cm^{-1} are calculated to arise mostly from the ground state modes at 1023 and 995

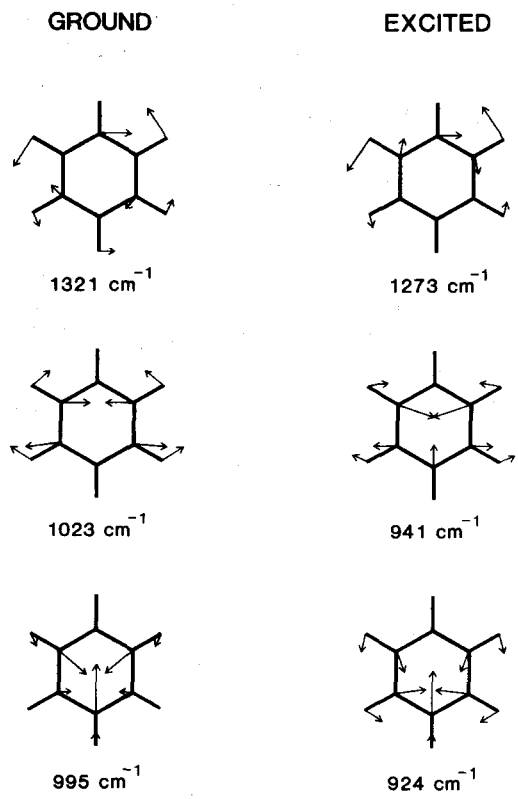

FIG. 7. Comparison of in-plane normal modes for the phenol ground ($^1A_1$) and excited ($^1B_2$) state undergoing strong alteration. The displacement correspond to 80 times the zero-point motions and H displacements are further weighted by $(m_H/m_C)^{1/2}$ and X atom (mass = 17.01 amu) displacement by $(m_X/m_C)^{1/2}$. Calculated frequencies are shown below each mode.

cm^{-1}, respectively. The mode pictures in Fig. 7 (middle) and mode decomposition calculations show that the mode at higher frequency has large Q''_{12} admixture, whereas its ground state counterpart (1023 cm^{-1}) in addition has large Q''_{18a} character. Q''_{12} has ring angle deformation character and Q''_{18a} contains mixed hydrogen and carbon e_{1u} angle deformation character and Q''_{18a} contains mixed hydrogen and carbon e_{1u} motions.[29] The lower frequency mode in both the excited (924 cm^{-1}) and the ground (995 cm^{-1}) state is predicted to be predominantly Q''_1 (a_{1g} ring breathing mode) but the atomic displacements are radically different in the two states (Fig. 7, bottom).

A brief comparison between the force field predictions and the major modes observed in the 2750 Å band system of phenol is instructive. The two-photon spectrum is dominated by the band at 1568 cm^{-1},[20] which by analogy to the appearance of the benzene two photon spectrum is clearly indicative of a mode containing large Q'_{14} character. As mentioned above, the force field does in fact attribute pure benzene Q'_{14} character to this mode. The principal Franck-Condon (FC) band in the $^1B_2 \leftarrow {}^1A_1$ absorption system is at 934 cm^{-1} and the corresponding mode calculated at 924 cm^{-1} is predominantly Q''_1 of benzene, the dominant Franck-Condon mode in the analogous $^1B_{2u} \leftarrow {}^1A_{1g}$ benzene spectrum. Finally, in phenol there are two medium intensity bands observed at 776 and 464 cm^{-1} above the origin (calculated at 747 and 436 cm^{-1}, respectively). The force field attributes large Q''_{6a} (e_{2g} ring distortion) character to the latter mode but substantial Q''_1 and Q''_{12} character to the former mode. Modes originating in Q''_1, Q''_{6a}, and Q''_{12} are always active vibrations in L_b spectra of monosubstituted benzenes.

BBW's extensive analysis of the one-photon spectrum established that after the strong origin band the spectrum was dominated by two fundamentals at 935 and 783 cm^{-1}, respectively; these are the same modes as the 934 and 776 cm^{-1} bands in the two photon spectra. Clearly, the normal coordinate Q_{14} character does not serve as a significant route to intensity in the L_b one-photon spectrum but Q_{12}, Q_1, and Q_{6a} do. The force field and decomposition calculations provide good explanations for the activity of these phenol fundamentals.

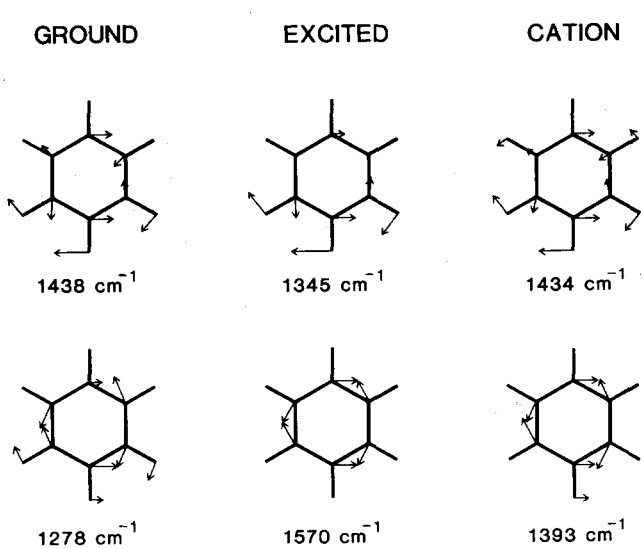

FIG. 8. Comparison of in-plane normal modes for the phenol ground ($^1A_1$) excited ($^1B_2$) state and cation ground ($^2B_1$) state undergoing strong alteration. The displacements correspond to 80 times the zero-point motions and H displacements are further weighted by $(m_X/m_C)^{1/2}$ and X atom displacements by (m_X/m_C).$^{1/2}$ Calculated frequencies are shown below each mode.

B. Cation ground state

Most of the calculated cation modes strongly resemble the neutral molecule modes in composition as evidenced by comparisons of the expansions in Table V with those of Tables III and IV. Only two modes undergo appreciable alteration in the ion relative to the neutral excited state (Fig. 8). Both modes possess b_2 symmetry. One is calculated at 1434 cm^{-1} in the ion with the parent mode in the excited state at 1345 cm^{-1} and the corresponding ground state mode at 1438 cm^{-1}. All three modes are composed almost exclusively of the benzene modes Q''_{19b} and Q''_3 but the relative amounts vary. In accordance with the closeness of the calculated neutral ground and ion ground state frequencies, the 1434 and 1438 cm^{-1} modes have very similar expansion coefficients, but the excited state mode is different and the mode alteration is therefore solely associated with the excited state. The other b_2 mode of interest is calculated at 1393 cm^{-1} in the ion with the parent mode in the excited state at 1570 cm^{-1} and the corresponding mode in the ground state

at 1278 cm^{-1}. These modes possess almost pure benzene Q''_{14} character and there is an increase in purity as the frequency increases and the carbon–hydrogen rocking character decreases (Fig. 8). The composition of the 1393 cm^{-1} cation mode is intermediate between the analogous neutral phenol ground and excited state modes as is its frequency.

The strongest band in the photoelectron spectrum obtained upon ionization out of the S_1 0–0 band occurs at 207 meV (1669 cm^{-1}), Fig. 4. The force field attributes the mode responsible for this band to be almost entirely benzene Q''_{8a}. The implication is that the main Franck–Condon coordinate for cation excitation is Q_{8a}. Inspection of the mode form for Q''_{8a}[29] as well as the more elaborate calculations on phenol including the additional OH internal coordinates indicate that this mode has some OH bending character. The prominent observation of ν_{8a} hence implies that the HOC angle changes upon removal of the π electron.

When the photoelectron spectrum is obtained via excitation of the 476 cm^{-1} band in S_1, a strong four-membered progression of frequency 516 cm^{-1} results (Fig. 4). The mode calculations indicate that both the 476 cm^{-1} excited neutral and 516 cm^{-1} cation vibronic levels (calculated at 436 and 479 cm^{-1}, respectively) are almost entirely the benzene mode Q''_{6a}. The simple appearance of the photoelectron spectrum combined with the Franck–Condon principle verifies that the 516 cm^{-1} level is largely described by Q''_{6a}.

On the other hand, a very complex spectrum results from excitation of the 975 cm^{-1} vibronic level of S_1. Photoelectron fundamental bands at 121 (1024 cm^{-1}), 150 (1210 cm^{-1}), and at 173 meV (1395 cm^{-1}) are strongly observed. The rationalization provided by the calculations is that the excited vibrational level in S_1 is a mixed mode containing both Q''_{9b} and Q''_{18b} characteristics. The first two transitions (calculated at 1037 and 1187 cm^{-1}, respectively) are actually predicted to involve modes containing substantial Q''_{18b} and Q''_{9b} character. The 1395 cm^{-1} mode matches ν_{14} in frequency but is actually more likely to be yet another mode containing Q''_{18b} or Q''_{9b} character as for example the b_2 mode calculated at 1321 cm^{-1}.

Lastly, a progression is observed at 101 meV (815 cm^{-1}) in the photoelectron spectrum excited from the 783 cm^{-1} vibronic level of S_1. According to the calculations the 783 cm^{-1} excited and 815 cm^{-1} cation vibronic levels (calculated at 747 and 801 cm^{-1}, respectively) are both heavily scrambled a_1 symmetry modes containing Q''_{18a}, Q''_{12}, Q''_{1}, and Q''_{6a} character.

The photoelectron spectrum of phenol-d_5 provides a fairly stringent test of the cation force field. We will only discuss in detail the spectrum generated by initial excitation of the S_1 0–0 band. The spectrum (Fig. 5) is marked by a strong origin band followed by two intense bands at 105 (847 cm^{-1}) and at 196 meV (1581 cm^{-1}). The latter band is the strongest feature in the spectrum. Two interpretations are possible, the first that the 196 meV band represents the overtone of 105 meV, with strong anharmonicity. The second, that the 105 and 196 meV bands represent two distinct fundamentals. The force field clearly favors the latter interpretation, predicting the 196 meV band to be equivalent to the strong 1669 cm^{-1} band in the calculated C_6H_5OH cation spectrum which remains virtually unperturbed. The overtone assignment would also require an unusual FC envelope. As discussed above, the 1669 cm^{-1} mode is largely Q''_{8a} with unknown degree of OH bending character. There is a less strongly active fundamental at 150 meV (1210 cm^{-1}) in $C_6H_5OH^+$ which the force field assigns as Q''_{9a}. However, ring deuteration strongly perturbs this mode, shifting it to the 850 cm^{-1} region according to the calculations. Thus the prominant fundamental (possibly a doublet) in the spectrum of $C_6D_5OH^+$ at 105 meV (847 cm^{-1}) is interpreted as being derived from Q''_{9a}. The force field is thus capable of providing an interpretation of the major spectral features in the $C_6D_5OH^+$ spectrum. Ionization from other excited state levels of phenol-d_5 may be understood and analyzed via the mode decomposition schemes as described above for the parent species.

IV. CONCLUDING REMARKS

The photoionization spectra of phenol obtained in this work fully confirm that the MPI-PES technique is an extremely powerful method for obtaining vibrational information about molecular ions.[17,18] It is just as evident, however, that the detailed interpretation of these spectra in terms of fundamental frequencies and mode forms represents a very difficult task. Accurate force fields for the ground, excited, and cation states are essential in this endeavor. Such force fields of medium-sized molecules cannot yet be established solely from electronic structure calculations, and there are unfortunately just too few fundamentals observed for the cation to create a highly accurate force field empirically. Spectra of additional isotopic phenols or spectra obtained via different intermediate states could alleviate this problem. However, the alternative perturbation model utilized here does provide a reasonable description of the cation modes and the appearance of the ionization spectra. In particular, the capability of the model to elucidate the differences in C_6H_5OH between the simple, diagonal ($\Delta v = 0$) spectra obtained from photoionization via the 0–0 or 476 cm^{-1} band of S_1 and the complicated spectrum obtained by excitation of the 975 cm^{-1} band, is noteworthy. Also, it was inferred from the observation of ν_{8a} and the calculated mode forms that the HOC angle should change even though the ionization is out of the π-electron system. The optimized geometries show an increase in the HOC angle from 105.3° to 112.0° from neutral to cation.[30(b)] This calculated result supports our claim that the perturbation model does represent the major vibrational features well.

ACKNOWLEDGMENTS

We would like to thank Wolfgang Henke and David Scholl for several helpful criticisms regarding inversion of TOF photoelectron data. We gratefully acknowledge financial support from the National Science Foundation (LG) and from the Donors of the Petroleum Research Fund, administered by the American Chemical Society (KK-J). We also acknowledge a generous grant of computer time from the Rutgers Center for Computer and Information Services. S.L.A., C.-F.Z., and R.N.Z. thank the Air Force Office of

Scientific Research (contract #AFOSRF49620-83-C-0033).

[1]G. Herzberg, *Infrared and Raman Spectra of Polyatomic Molecules* (Van Nostrand, New York, 1945).
[2]E. B. Wilson, Jr. J. C. Decius, and P. C. Cross, *Molecular Vibrations* (McGraw–Hill, New York, 1955).
[3]S. Califano, *Vibrational States* (Wiley, New York, 1976).
[4]*Vibrational Spectra and Structure*, edited by J. R. Durig (Elsevier, Amsterdam, 1972), Vol. 1.
[5]T. A. Miller and V. E. Bondybey, Appl. Spectrosc. Rev. **18**, 105 (1982).
[6]D. Klapstain, J. P. Maier, and L. Misev, in *Molecular Ions: Spectroscopy, Structure and Chemistry*, edited by T. A. Miller and V. E. Bondybey (North-Holland, Amsterdam, 1983).
[7]M. A. Johnson, C. R. Webster, and R. N. Zare, J. Chem. Phys. **75**, 5575 (1981); M. A. Johnson, R. N. Zare, J. Rostas, and S. Leach, *ibid.* **80**, 2407 (1984).
[8]T. Oka, Phys. Rev. Lett. **45**, 531 (1980); Philos. Trans. R. Soc. London Sect. A **303**, 543 (1981); *Laser Spectroscopy* (Springer, New York, 1981), p. 320.
[9]P. Bernath and T. Amano, Phys. Rev. Lett. **48**, 20 (1982); M. Wang, P. Bernath, and T. Amano, J. Chem. Phys. **77**, 693 (1982).
[10]C. S. Gudeman, M. H. Begemann, J. Pfaff, and R. J. Saykally, Phys. Rev. Lett. **50**, 727 (1983); J. Chem. Phys. **78**, 5837 (1983); M. H. Begemann, C. S. Gudeman, J. Pfaff, and R. J. Saykally, Phys. Rev. Lett. **51**, 554 (1983); E. Schäfer, M. H. Begemann, C. S. Gudeman, and R. J. Saykally, J. Chem. Phys. **79**, 3159 (1983).
[11]W. H. Wing. G. A. Ruff, W. E. Lamb, Jr., and J. J. Spezeski, Phys. Rev. Lett. **36**, 1488 (1976); J.-T. Shy, J. W. Farley, W. E. Lamb, Jr., and W. H. Wing, *ibid.* **45**, 535 (1980); J.-T. Shy, J. W. Farley, and W. H. Wing, Phys. Rev. A **24**, 1146 (1981).
[12]A. Carrington, J. A. Buttershaw, and R. A. Kennedy, Mol. Phys. **45**, 753 (1982).
[13]D. W. Turner, C. Baker, A. D. Baker, and C. R. Brundle, *Molecular Photoelectron Spectroscopy* (Wiley, New York, 1970).
[14]J. W. Rabalais and R. J. Colton, J. Electron Spectrosc. **1**, 83 (1972); T. P. Debies and J. W. Rabalais, *ibid.* **1**, 355 (1972/73); J. W. Rabalais, *Principles of Ultraviolet Photoelectron Spectroscopy* (Wiley, New York, 1977).
[15]K. Kimura, S. Katsumata, Y. Achiba, T. Yamazaki, and S. Iwata, *Handbook of He I Photoelectron Spectra of Fundamental Organic Molecules* (Halsted, New York, 1981).
[16]K. Siegbahn, C. Nordling, A. Fahlman, R. Nordberg, K. Hamrin, J. Hedman, G. Johansson, T. Bergmark, S.-E. Karlsson, I. Lindgren, and B. Lindberg, Nova Acta R. Soc. Scient. Upsal. **4**, 20 (1967); K. Siegbahn, C. Nordling, G. Johansson, J. Hedman, P. F. Heden, K. Hamrin, U. Gelius, A. T. Bergmark, L. O. Werme, R. Manne, and Y. Baer, *ESCA—Applied to Free Molecules* (North-Holland, Amsterdam, 1969).
[17](a) J. T. Meek, S. R. Long, and J. P. Reilly, J. Phys. Chem. **86**, 2809 (1982); (b) S. R. Long, J. T. Meek, and J. P. Reilly, J. Chem. Phys. **79**, 3206 (1983).
[18]S. L. Anderson, D. M. Rider, and R. N. Zare, Chem. Phys. Lett. **93**, 11 (1982); J. L. Durant, D. M. Rider, S. L. Anderson, F. D. Proch, and R. N. Zare, J. Chem. Phys. **80**, 1817 (1984). S. L. Anderson, G. Kubiak and R. N. Zare, Chem. Phys. Lett. **105**, 22 (1984).
[19]H. D. Bist, J. C. D. Brand, and D. R. Williams, J. Mol Spectrosc. **21**, 76 (1966); **24**, 402, 413 (1967).
[20]R. P. Rava and L. Goodman, J. Am. Chem. Soc. **104**, 3815 (1982).
[21]M. L. Fraser-Monteiro, L. Fraser-Monteiro, J. DeWit, and T. Baer, J. Phys. Chem. **88**, 3622 (1984).
[22]M. A. Duncan, J. G. Dietz, and R. E. Smalley, Chem. Phys. **44**, 415 (1979); P. C. Engelking, Chem. Phys. Lett **74**, 207 (1980), W. W. Harrison, D. M. Rider, and R. N. Zare, Int. J. Mass. Spectrom. Ion Proc. (submitted).
[23]P. Cossee and J. H. Schachtschneider, J. Chem. Phys. **44** 97 (1960).
[24]T. Pedersen, N. W. Larsen, and L. Nygaard, J. Mol. Struct. **4**, 59 (1969).
[25]A. Langseth and B. P. Stoicheff, Can. J. Phys. **34**, 350 (1956).
[26]R. A. Kydd, Ph.D. thesis, University of British Columbia, 1969.
[27]M. J. Robey and E. W. Schlag, J. Chem. Phys. **67**, 2775 (1977).
[28]R. L. Redington, J. Mol. Spectrosc. **65**, 171 (1977).
[29]K. Krogh-Jespersen, R. P. Rava, and L. Goodman, J. Phys. Chem. **88**, 5503 (1984).
[30](a) The $2p(\pi)$ coefficients are taken from an *ab initio* Hartree–Fock calculation with the STO-3G basis set on the optimized phenol geometry (C_s symmetry; HF/STO-3G//STO-3G). (b) K. Krogh-Jespersen (unpublished results).
[31]F. A. Cotton, *Chemical Applications of Group Theory* (Wiley, New York, 1971).
[32]J. R. Lombardi, R. Wallenstein, T. W. Hänsch, and D. M. Friedrich, J. Chem. Phys. **65**, 2537 (1976).
[33]F. Duschinsky, Acta. Physico Chem. URSS **1**, 551 (1937); G. Orr and G. J. Small, J. Chem. Phys. **2**, 60 (1973).